Pure Apodized Phase-Shifted Fiber Bragg Gratings Fabricated by a Two-Beam Interferometer With Polarization Control

Kai-Ping Chuang, Yinchieh Lai, and Lih-Gen Sheu

***Abstract*—A new technique based on a two-beam interferometer with polarization control for fabricating advanced fiber Bragg grating (FBG) devices is demonstrated. By simultaneously rotating the angle of the half-wave plate, pure apodized and π-phase-shifted FBGs can be fabricated in a single scan.**

***Index Terms*—Apodization of fiber Bragg grating, fiber Bragg grating (FBG), phase-shifted fiber Bragg grating.**

I. Introduction

In RECENT years the fiber Bragg grating (FBG) devices have found a lot of applications in fiber communication and fiber sensing. In particular, they can act as the channel multiplexer–demultiplexers or the dispersion compensators in dense wavelength-division-multiplexing systems, in which the requirements for the optical filter properties are very stringent. The spectral shape of these optical filters needs to have a steep edge, very low sidelobes, and a flat top with very little ripples. For FBG filters to meet these requirements, it is important to apodize the FBG structure such that its dc index change remains a constant across the whole grating (pure apodization). For more advanced FBGs like dispersionless FBGs, multiple π-phase shifts are also required. In the literature, several fabrication methods for these so-called pure apodized FBGs have been developed. The double-ultraviolet (UV) exposure methods [1]–[3] need a two-stage exposure process and the variable-diffraction-efficiency phase mask method [4] needs a special designed mask. The phase mask dithering method [5] adopts mask dithering to achieve a constant dc refractive-index change during a single scan, but it will more easily induce extra vibration for the interferometric control of the relative position between the fiber and the phase mask. Recently, it was shown that apodized FBGs with constant average index and phase shifts can be fabricated by using a phase mask polarization control method [6]. However, in this method, the FBG length is limited by the size of the phase mask and the precision adjustment of the fiber-to-phase-mask distance and the polarizer alignment are needed.

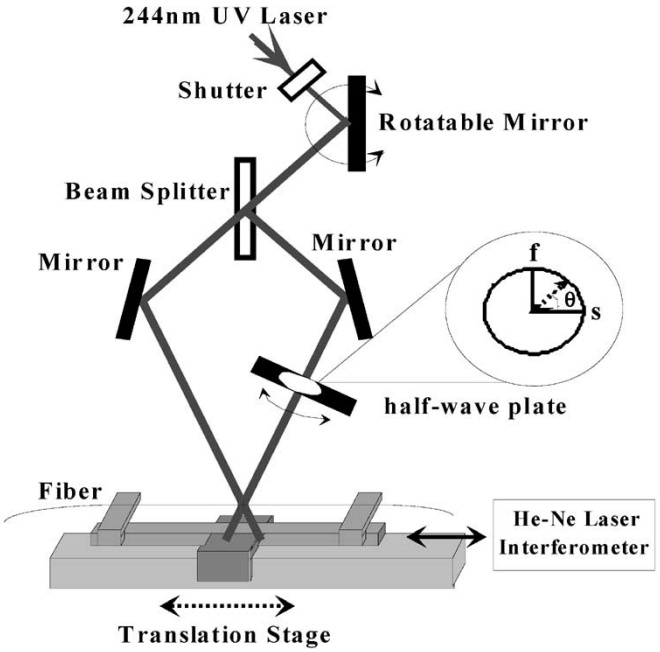

Fig. 1. Schematic diagram of FBG fabrication system.

In the present letter, we propose and demonstrate a new method which is capable of fabricating FBGs with not only pure apodization profiles but also π-phase shifts. This method is based on the two-beam interferometer technique with the polarization control on one of the interfering beams. The FBG is exposed by a step-scan exposure method and the pure apodization profile as well as π-phase shifts can be achieved in a single scan.

II. Experimental Setup and Working Principle

The experimental setup is illustrated in Fig. 1. A frequency-doubled argon-ion laser launches a continuous-wave 244-nm single-polarization UV beam into a two-beam interferometer with a half-wave plate in one of the two interfering beams. The fiber is placed in a holder mounted on a translation stage composed of a linear motor stage and a piezoelectric translator stage with subnanometer (sub-nm) resolution. A He–Ne laser interferometer (Agilent 5529A system) with 2.5-nm position measurement resolution directly from the instrument is used for monitoring the fiber position. Sub-nm resolution can be achieved by

Manuscript received August 25, 2003; revised November 6, 2003. This work was supported in part by the National Science Council of the Republic of China under Contract NSC 91-2215-E-009-026, the Ministry of Education of the Republic of China, and in part by the Lee Center at National Chiao-Tung University.

K.-P. Chuang and Y. Lai are with the Institute of Electro-Optical Engineering, National Chiao-Tung University, Hsinchu 300, Taiwan, R.O.C. (e-mail: yclai@mail.nctu.edu.tw).

L.-G. Sheu is with the Department of Electronic Engineering, Van Nung Institute of Technology, Tao-Yuan 320, Taiwan, R.O.C. (e-mail: slg2018@cc.vit.edu.tw).

Digital Object Identifier 10.1109/LPT.2004.823762

time-averaging a certain number of the sample points. A shutter is placed at the entrance of the setup in order to control the UV exposure flux. A rotating reflecting mirror which controls the interference angle is used to change the period of the interference fringes. Because of the special symmetrical optical design, the induced angle changes for both beams will be the same and, thus, the UV standing wave pattern will not be angle-tilted with respect to the fiber. Although the overlap area between the interfering beams will move orthogonally to the fiber, we do not need to redo the alignment of the setup when the changed angle is small since the position sensitivity is less severe. Even when the changed angle is large, a simple one-dimensional translation can be easily implemented to adjust the fiber position. This feature is quite useful for establishing a flexible exposure platform. The function of the half-wave plate is to rotate the polarization of the UV beam. It has been well known that for a general azimuthal angle θ between the input polarization and the wave-plate axis, the half-wave plate will rotate the beam polarization by an angle 2θ. Since the two interfering beams have the same linear polarization before passing through the wave plate and the field components of orthogonal polarizations will not interfere, the maximum refractive-index modulation amplitude is obtained at $\theta = 0^\circ$ and zero modulation amplitude occurs at either $\theta = -45^\circ$ or 45°. The orthogonal polarization field component generated by the polarization rotation of the wave plate has no contribution to the ac-modulation index, but will contribute to the dc-index change. To be more explicit, the ac-refractive-index modulation amplitude will be a $\cos^2(2\theta)$ function according to a simple derivation. Therefore, with this setup, the ac-index change of the exposed FBG section can be adjusted by changing the angle θ. Moreover, by switching the fast and the slow axes of the wave plate with a 90° angle rotation, we can also keep the output polarization the same but introduce an additional π-phase shift on to the UV beam. In this way, we can easily and accurately produce π-phase-shifted interference fringes on the fiber for exposing the π-phase-shifted FBGs.

In our proposed method, the FBG is fabricated by an overlap-step-scan exposure approach [7]. We expose the fiber section-by-section and the adjacent sections overlap strongly to smooth out the random errors. The exposure time for each section is kept the same and the ac-index modulation of the FBG is controlled by changing the rotation angle of the half-wave plate. The dc-index change for each section exposure will be the same no matter what the angle of the wave plate is, as long as the exposure time for each section is fixed constant. One intuitive way to understand this is to notice that the total UV flux for each section exposure is always the same, independent of the wave-plate angle. When the ac-index modulation is smaller (larger), the dc-index change created by the orthogonal field component becomes larger (smaller) and the net dc-index change remains the same as long as the exposure time is fixed. In this way, we can achieve a flat dc-index change, as illustrated in Fig. 2(a) after the exposure scan, as long as the step-scan size is much smaller than the beam width of the exposure UV beam.

III. Experimental Results

In order to demonstrate that our new method can be truly applicable, we first expose single-section FBGs with different rotation angles of the wave plate and measure their

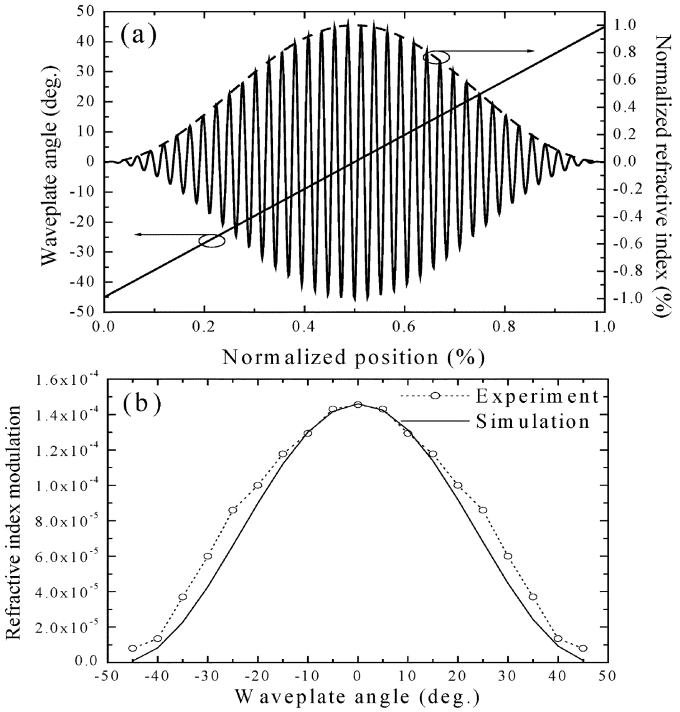

Fig. 2. (a) Relation of the half-wave plate angle and the refractive index modulation amplitude along the FBG position and (b) experimental and theoretical results for the refractive index modulation versus the rotation angle of the half-wave plate.

corresponding refractive index modulation. By theoretically calculating the corresponding visibility for each rotating angle of the half-wave plate to obtain the theoretical value of the refractive index modulation versus the rotation angle of the half-wave plate, in Fig. 2(b) we verify that the experimental results match the theoretical predictions well. However, in the figure, it seems to show a systematic deviation between the theoretical curve and the experimental points. One of the possible causes is the nonlinear behavior of the refractive index modulation versus the exposed energy [8]. We have tried to characterize the nonlinear behavior from our measurement data and to check numerically whether the deviation caused by the nonlinear effects can be significant.[1] We find that for the FBGs with symmetric apodization profiles, the impacts are less significant (only sidelobes are larger). However, for FBGs with asymmetric apodization profiles (like the dispersionless FBGs), the impacts will be more significant (the spectral shape may be even changed). In principle, in order to achieve more accurate control of the induced index modulation and to avoid the bad impacts of the nonlinear effects, we can incorporate this nonlinear behavior in the design with a careful calibration based on the measured grating visibility versus the wave-plate angle for the fixed exposure energy.

We then proceed to fabricate a pure apodized FBG with a cosine^2 apodization function. The FBG is formed in a photosensitive fiber after 100-section sequential writing with a total grating length about 5 cm. It is fabricated by the overlap-step-scan exposure setup with the exposed UV beam diameter $= 5.2$ mm and the fiber scan step $= 535$ μm. We uniformly rotated the half-wave plate azimuth angle from

[1]Thanks to the comments from one of the reviewers.

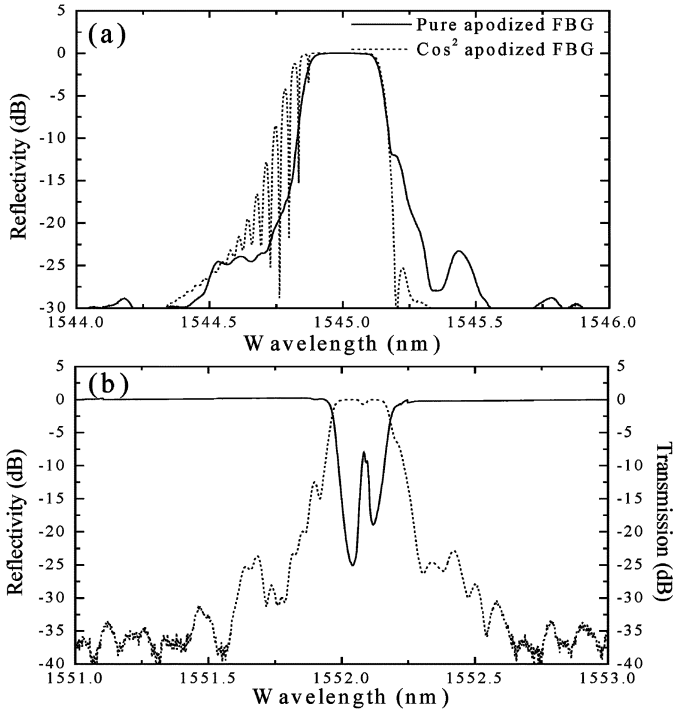

Fig. 3. (a) Reflection spectra of the $\cos^2$ pure apodized (experiment) and ordinarily apodized (simulation) FBGs and (b) reflection and transmission spectra of a π-phase-shifted FBG.

$\theta = -45^\circ$ to 45° during the exposure scan to produce the required apodization. For comparison, we also show the theoretical reflection spectrum for the FBG with the same cosine^2 apodization function but also with a nonconstant dc index change (half of the ac-index envelope) as in ordinarily apodized FBGs. In Fig. 3(a), we show the reflection spectra of both gratings. One can see that the cosine^2 "ordinarily" apodized FBG (dotted line) will have much higher sidelobes than the purely apodized FBG (real line) on the short wavelength side. The sidelobes of the "ordinarily" apodized cosine^2 FBG are mainly due to the self-chirp caused by the nonuniform dc-index along the grating length [2]. This is the main reason why pure apodization is usually needed for achieving high performance.

In Fig. 3(b), we show an example of the fabricated π-phase-shifted FBGs. It is a 3-cm-long FBG with a raised-cosine^2 shape and the added π-phase shift is created by rotating an additional 90° angle of the half-wave plate after half of the scan. As expected, the π-phase shift induces a narrow transmission peak in the middle of the stopband. The measurement resolution of the transmission peak is limited by the 0.01-nm resolution of our optical spectrum analyzer. Multiple π-phase-shifted FBGs also can be fabricated easily with the present method. This kind of π-phase-shift fabrication technique should be very useful for producing advanced FBG devices as well as for the applications of distributed feedback fiber lasers.

In the proposed method both the s-polarized and p-polarized UV beams in different ratios have been utilized for FBG fabrication. In [9], it has been shown that the UV polarization is the dominant cause of birefringence in the UV-induced index change. The induced birefringence of our fabricated FBGs is experimentally estimated to be 1%–2% of the index modulation if the s-polarization UV beam is used. This is in reasonable agreement with the results reported in [9]. The induced birefringence by the p-polarized UV beam can be smaller by a factor 3–10 (depending on the fiber type), also according to [9]. One of the possible impacts of such birefringence on our scheme is to make the induced dc- and ac-index profiles deviated from what we have anticipated. However, through simple numerical simulation, we find that if the 2% birefringence is assumed, its effects on the spectral reflection profiles of our test FBG samples (through the index profile deviation) are very small and can be safely neglected. Nevertheless, if the fabricated FBGs have reflectivity ripples or group delay ripples within the stopband, then the birefringence may transform these ripples into polarization-dependent-loss ripples and polarization-mode-dispersion ripples. We are currently investigating these effects more carefully and the results will be reported elsewhere.

IV. Conclusion

We have demonstrated that pure apodization and π-phase-shifted FBGs can be achieved through the combination of a novel two-beam interferometer with polarization control and the overlap-step-scan exposure method. The required ac refractive index modulation as well as π-phase shifts can be achieved easily by rotating the half-wave plate during the scan and the dc-index change can be fixed at a constant simultaneously. This new technique should have the great potential to become a powerful tool for fabricating complicated FBG structures for different application purposes.

References

[1] B. Malo, S. Theriault, D. C. Johnson, F. Bilodeau, J. Albert, and K. O. Hill, "Apodised in-fiber Bragg grating reflectors photoimprinted using a phase mask," *Electron. Lett.*, vol. 31, pp. 223–225, 1995.

[2] H. Singh and M. Zippin, "Apodized fiber Bragg gratings for DWDM applications using uniform phase mask," in *Proc. 24th Eur. Conf. Optical Communication*, vol. 1, Madrid, Spain, 1998, pp. 189–190.

[3] C. Yang and Y. Lai, "Apodised fiber Bragg gratings fabricated with uniform phase mask using low cost apparatus," *Electron. Lett.*, vol. 36, pp. 655–657, 2000.

[4] J. Albert, K. O. Hill, B. Malo, S. Theriault, F. Bilodeau, D. C. Johnson, and L. E. Erickson, "Apodization of the spectral response of fiber Bragg gratings using a phase mask with variable diffraction efficiency," *Electron. Lett.*, vol. 31, pp. 222–223, 1995.

[5] W. H. Loh, M. J. Cole, M. N. Zervas, S. Barcelos, and R. I. Laming, "Complex grating structures with uniform phase masks based on the moving-scanning beam technique," *Opt. Lett.*, vol. 20, pp. 2051–2053, 1995.

[6] J. B. Jensen, M. Plougmann, H.-J. Deyerl, P. Varming, J. Hubner, and M. Kristensen, "Polarization control method for ultraviolet writing of advanced Bragg gratings," *Opt. Lett.*, vol. 27, pp. 1004–1006, 2002.

[7] L. G. Sheu, K. P. Chuang, and Y. Lai, "Fiber Bragg grating dispersion compensator by single-period overlap-step-scan exposure," *IEEE Photon. Technol. Lett.*, vol. 15, pp. 939–941, July 2003.

[8] H. Patrick and S. L. Gilbert, "Growth of Bragg gratings produced by continuous-wave ultraviolet light in optical fiber," *Opt. Lett.*, vol. 18, pp. 1484–1486, 1993.

[9] T. Erdogan and V. Mizrahi, "Characterization of UV-induced birefringence in photosensitive Ge-doped silica optical fibers," *J. Opt. Soc. Amer. B*, vol. 11, pp. 2100–2105, 1994.